Carbon 1s Excitation Spectroscopy of Propyne, Trifluoropropyne, and Propargyl Alcohol

Liu Yang and John J. Neville*

Department of Chemistry and Centre for Laser, Atomic and Molecular Sciences, University of New Brunswick, Fredericton, NB, E3B 4R8, Canada

Received: May 27, 2005; In Final Form: October 10, 2005

The C 1s excitation spectra of propyne (HC_2CH_3), 3,3,3-trifluoropropyne (HC_2CF_3), and propargyl alcohol (HC_2CH_2OH) have been studied using synchrotron radiation and ion time-of-flight mass spectrometry. Discrete peaks below the carbon 1s ionization thresholds are compared and assigned, aided in part by ab-initio calculations incorporating an explicit C 1s hole. Calculated C 1s ionization potentials are in good agreement with previously reported experimental values. Calculated absolute excitation energies consistently underestimate the transition term values, but calculated relative excitation energies and intensities are in good agreement with the experimental results. The spectra are dominated by intense C 1s → π^* transitions. In the case of propyne, C 1s excitations from each of the three chemically inequivalent carbon atoms are observed. The effect of electronegative substitution is found to be different for the C 1s → Rydberg transitions than for transitions to unoccupied valence levels, with Rydberg transition energies shifting with changes in the C 1s ionization potentials but valence transition energies showing only small changes with electronegative substitution. The C 1s ($3a_1$,$4a_1$) → π^* (6e) transitions of trifluoropropyne are shifted to lower energy relative to propyne even though the electronegative fluorine atoms cause a significant shift to higher energy in the corresponding C 1s IPs.

Introduction

Inner-shell excitation spectroscopy of atomic and molecular systems has been investigated extensively and proven to be a useful tool to elucidate the electronic structure of free molecules.[1,2] Inner-shell excitation energies exhibit chemical shifts that reflect their electronic environment, hence the widespread use of inner-shell spectroscopy as an analytical tool to characterize materials. Inner-shell excitation energies reflect the inner-shell MO from which the electron is promoted, the upper valence or Rydberg orbital that becomes singly occupied with inner-shell excitation, and the extent of interaction and relaxation that occurs between the two.

Unlike the valence electrons where the electron density is delocalized among bonding atoms, the inner-shell electrons are usually highly localized around specific atoms. Thus inner-shell excitation spectroscopy can be used to investigate the chemical environment at specific atomic sites. Current synchrotron sources and X-ray optics make experimental differentiation of inner-shell excitations from chemically similar but inequivalent atoms readily achievable. It is of interest to explore the relationship between the site of inner-shell excitation and the extent of interaction between the inner-shell hole and the singly occupied upper level as well as the degree of electronic relaxation upon formation of the inner-shell hole. Site-selective inner-shell excitation spectroscopy should also serve as an excellent probe of the effects of chemical substitution and other local changes not only at the site of the change but also throughout the molecule.

Propyne, one of the simplest hydrocarbons with three inequivalent carbon atoms, is an ideal candidate to be used to investigate the electronic structure of the three carbons by core excitation spectroscopy. There has been much work investigating the isomerization and photodissociation of propyne in the vacuum ultraviolet, because of its role in the formation of simple aromatics and soot during the oxidation of aliphatic hydrocarbons.[3−6] In contrast, there has been comparatively little investigation of the inner-shell ionization or excitation of propyne. In 1975, Cavell measured the carbon 1s photoelectron spectrum of propyne, observing a single asymmetric peak.[7] Although assigned to the three inequivalent carbons in propyne, the modest resolution prevented a definitive assignment. More recently, Sæthre et al. obtained the high-resolution carbon 1s photoelectron spectra of propyne, trifluoropropyne, and ethynylsulfur pentafluoride.[8] In their ionization spectra, the three chemically inequivalent carbons of propyne are clearly resolved and distinguished by distinct vibrational structure. The C 1s electron energy loss spectra (EELS) of propyne, trifluoropropyne, and propargyl alcohol recorded by Hitchcock et al. show only a single peak for C 1s → π^* excitation from the ethynyl carbons and failed to resolve the Rydberg transitions.[2,9,10] Ishii and Hitchcock compared the C 1s EELS spectrum of propargyl alcohol with other alcohols to investigate the substitution effects and were only able to assign the C 1s → valence orbital transitions.[9] The EELS spectra of propyne and propargyl alcohol have been discussed by Stöhr[2] in the context of shifts in the dominant spectral features among related molecules, but complete spectral assignments were not provided.

Recently, the C 1s excitation spectrum of trifluoropropyne at good resolution was reported by Okada et al.[11] They assigned the C 1s → π^* and C 1s → σ^* transitions on the basis of the anisotropy parameters of fragment ions obtained by an angle-resolved mass spectrometer. The C 1s → Rydberg transitions were assigned on the basis of the experimental term values and quantum defects. However, the ionization potentials used to obtain the term values differ from the most recent experimental

* Corresponding author. E-mail: jneville@unb.ca.

10.1021/jp052823m CCC: $30.25
Published on Web 11/19/2005

IPs.[8] Furthermore, the energy scale differs by ~0.7 eV from Hitchcock's EELS spectrum.

Here we present C 1s excitation spectra of propyne, 3,3,3-trifluoropropyne, and propargyl alcohol to explore electronegative substitution effects on the chemical shifts of the core excitation transitions. Of particular interest is how substitution at one site in a molecule affects not only the excitation spectroscopy from the site of substitution, but excitations throughout the molecule. Ab-initio calculations are used to aid in the assignment of the spectra and to provide a picture of how the electronic structure of the target molecules changes with substitution and with creation of a C 1s hole at the various carbon centers in the molecule.

Methods

Experimental. The total-ion-yield (TIY) spectra of the gas-phase samples were recorded using a time-of-flight mass spectrometer (TOF) with a 20-cm drift tube for ion detection. Tunable, monochromatic synchrotron radiation was provided by the spherical grating monochromator bending magnet beamline (063)[12] of the Canadian Synchrotron Radiation Facility (CSRF), Synchrotron Radiation Center (SRC), University of Wisconsin-Madison. Trial measurements with entrance and exit slit settings of 10, 30, 50, and 100 μm were performed. Entrance and exit slit settings measuring 30 μm were found to give the best compromise between energy resolution and photon flux and were therefore used throughout this work. Measurements of the C 1s $\rightarrow \pi^*$ band of CO indicate that the energy resolution is about 60 meV at the C 1s edge with these slit settings.

The experimental chamber consisted of a time-of-flight mass spectrometer for cation detection, an electron detector, and an effusive gas jet. Details of the apparatus have been described previously.[13,14] The individual components were mounted on a six-way cross main chamber with the TOF and electron detector mounted opposite to each other and perpendicular to the direction of the photon beam. The effusive gas jet was mutually orthogonal to the TOF and the photon beam. An electric field of 500 V/cm was applied to the ionization region to extract electrons and ions to their corresponding detectors. The remaining voltages of the TOF were set to satisfy the Wiley−McLaren space-focusing condition.[15] The TIY detected in a fixed dwell time was recorded as a function of photon energy and normalized to sample pressure and incident photon flux. The photon flux was monitored using a Cu mesh. The signal was corrected for the variable response of the Cu with photon energy using the Ne TIY spectrum measured under identical conditions and the published Ne photoabsorption cross section.[16] The energy calibration was performed with the CO C 1s TIY spectrum by comparison to the peak positions reported by Saito et al.[17] The accuracy of the energy calibration is estimated to be ±0.10 eV.

The samples, propyne, propyne-*3,3,3-d*$_3$, 3,3,3-trifluoropropyne, and propargyl alcohol were all commercially available and used without further purification. The base pressure of the main chamber was 4×10^{-8} Torr. When sample gas was admitted from the sample line to the ionization cell, the pressure of the main chamber was maintained at about 4×10^{-6} Torr.

Computational. Ab-initio molecular orbital (MO) calculations were carried out to estimate the transition energies and intensities of the core hole states. First, the ground-state equilibrium geometries of propyne, trifluoropropyne, and propargyl alcohol were determined at the HF/6-311G(d,p) level using GAMESS.[18] These geometries were used for all subsequent calculations. The C 1s excitation energies and intensities (oscillator strengths) were then determined using Kosugi's GSCF3 program.[19] The calculations proceeded in three steps: first, a HF calculation of the ground state was performed; second, the C 1s ionized states were calculated with explicit consideration of the core hole; and finally, the C 1s excited states were obtained by the improved virtual orbital (IVO) method.[20] This approach accounts for the significant alterations in the electronic structure that occur due to relaxation of the valence shell MOs in the presence of the core hole. The differences in the total energy between the core ionized states and the ground state are the core ionization potentials (IPs). The final step yields the transition energies and intensities of the C 1s excitations. For the GSCF3 calculations, primitive basis functions were taken from (73/7) contracted Gaussian-type functions for carbon, fluorine, and oxygen, and (411) for hydrogen.[21] Polarization functions were added to carbon (ζ_d = 0.626), fluorine (ζ_d = 1.75), oxygen (ζ_d = 1.292), and hydrogen (ζ_p = 0.75).[22] The contraction schemes, indicating (s/p/d) functions, were (4111111/ 31111/1) for the C 1s excited carbon; (721/511/1) for the other carbon atoms, fluorine, and oxygen; and (411/1) for hydrogen. The diffuse functions proposed by Kaufmann et al.[23] were added to the C 1s excited carbon atom to describe 3s−4s, 3p−4p, and 3d−4d Rydberg orbitals: ζ_s = 0.075, 0.02530, 0.01141, 0.00589, and 0.00334; ζ_p = 0.0440, 0.01970, 0.01013, 0.00573, and 0.00349; and ζ_d = 0.02820, 0.01447, 0.00817, and 0.00496.

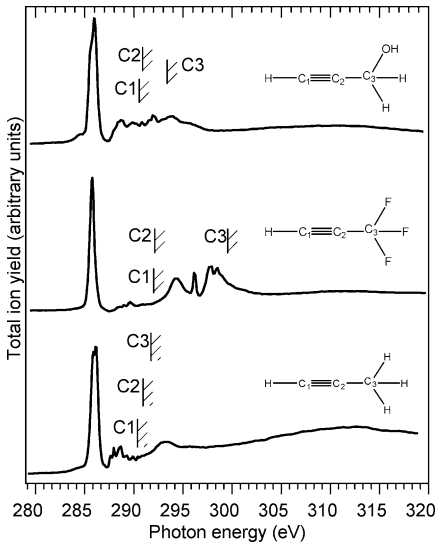

Figure 1. TIY spectra of propargyl alcohol (top), trifluoropropyne (middle), and propyne (bottom), in the 280−320 eV photon energy region. The hatched lines indicate the experimental C 1s IPs of propyne and trifluoropropyne[8] and the calculated IPs of propargyl alcohol.

Results and Discussion

Total Ion Yields.

The TIY spectra near the C 1s ionization thresholds of propyne, trifluoropropyne, and propargyl alcohol are shown in Figure 1. The hatched lines above the propyne and trifluoropropyne spectra are the reported experimental ionization potentials,[8] and those of propargyl alcohol are our calculated results. To simplify the discussion throughout this paper, for each molecule the terminal HC≡ ethynyl carbon is referred to as C1; the central ≡C− carbon is C2; and the terminal sp^3-hybridized carbon is referred to as C3, as shown in Figure 1. The C 1s spectra of the three target molecules are dominated by strong C 1s $\rightarrow \pi^*$ transitions, followed by a series of weaker Rydberg transitions. In trifluoropropyne, discrete excitations from the fluorinated carbon C3 are also relatively intense and

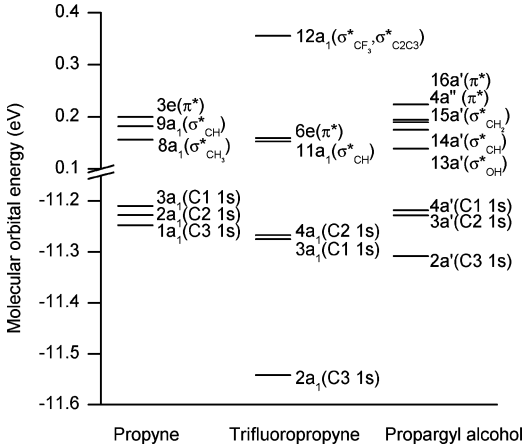

Figure 2. Energies of carbon 1s MOs and low-lying unoccupied valence MOs of propyne, trifluoropropyne, and propargyl alcohol in the ground state, from HF/6-311G(d,p) calculations.

shifted to higher photon energy in comparison with excitations from C1 and C2 in trifluoropropyne and with excitations from all three carbon centers in propyne and propargyl alcohol. This is attributable to the high electronegativity of fluorine, as will be discussed in more detail below.

The TIY spectra reported here are consistent with the previous EELS spectra of these molecules.[2,9,10] However, the much better energy resolution of the present data (60 meV vs ~500 meV) reveals considerably more spectral detail. In particular, individual Rydberg transitions are resolved, and the C 1s $\rightarrow \pi^*$ bands in propyne and propargyl alcohol reveal structure not evident in the previous work. The C 1s TIY spectrum of trifluoropropyne is consistent with the photoabsorption spectrum, recorded with similar energy resolution, recently reported by Okada et al.,[11] with the exception that the energy scale of the photoabsorption spectrum is shifted ~0.8 eV to lower energy in comparison with both the present data and the EELS spectrum.[10] Our proposed assignments of the trifluoropropyne spectrum also differ in some respects from those of Okada et al., as is discussed below.

Prior to examining the spectra of these molecules in detail, it is helpful to consider their respective ground-state electronic configurations. The HF/6-311G(d,p) energies of the ground-state C 1s and low-lying unoccupied valence molecular orbitals involved in C 1s-to-valence excitation in these molecules are shown in Figure 2. Propyne and trifluoropropyne have C_{3v} symmetry, while propargyl alcohol has C_s symmetry. The ground-state molecular orbital configuration of propyne is $(1a_1)^2(2a_1)^2(3a_1)^2(4a_1)^2(5a_1)^2(6a_1)^2(7a_1)^2(1e)^4(2e)^4(8a_1)^0(9a_1)^0(3e)^0$. The three lowest-energy orbitals are C3, C2, C1 1s orbitals, respectively, as shown in Figure 2. The HF/6-311G(d,p) calculations indicate the C 1s MOs are highly localized on individual carbon atoms. The three lowest-energy unoccupied MOs of propyne in the ground state are $\sigma^*_{CH_3}$ ($8a_1$), σ^*_{CH} ($9a_1$), and $\pi^*_{C1\equiv C2}$ (3e). The π^* orbitals also have some π_{C2-C3} bonding and $\sigma^*_{CH_3}$ antibonding character. In C_{3v} symmetry, the Rydberg-like orbitals are split into two sets: s, p_z, and d_{z^2} have a_1 symmetry, whereas p_x, p_y, d_{xy}, $d_{x^2-y^2}$, d_{xz}, and d_{yz} have e symmetry. Transitions from the a_1-symmetry C 1s orbitals to both a_1 and e symmetry orbitals are dipole allowed. However, because of the highly localized nature of the C 1s orbitals, transition intensities will only be significant to those valence orbitals with significant density on the core excited atom. For example, C 1s transitions from C1 and C2 to $\pi^*_{C1\equiv C2}$ (3e) are expected to be much more intense than transitions from C3 1s, while the reverse is expected for transitions to $\sigma^*_{CH_3}$ ($8a_1$). Also, although transitions to s, p, and d Rydberg-like orbitals are allowed within the symmetry of these molecules, consideration of these processes as quasi-atomic excitations generally provides a good qualitative prediction of the relative transition intensities. Therefore, among the Rydberg-like transitions, we expect C 1s $\rightarrow$ 3p to be most intense. The relative ground-state MO energies indicated in Figure 2 are expected to provide only a first-order estimate of the relative C 1s excitation energies, because electronic relaxation in the presence of the core hole is typically significant and will vary depending upon the extent of interaction between the core holes and the unoccupied valence or Rydberg orbitals. For example, the LUMO ($\sigma^*_{CH_3}$ ($8a_1$)) of propyne has lower energy than $\pi^*_{C1\equiv C2}$ (3e) in the ground state. However, $\pi^*_{C1\equiv C2}$ (3e) will have a larger overlap with the C1, C2 1s ($2a_1$, $3a_1$) orbitals; when the C1, C2 core holes are formed, the energy of $\pi^*_{C1\equiv C2}$ (3e) will be lowered more than the energy of the $\sigma^*_{CH_3}$ ($8a_1$) orbitals. Therefore, we expect that C1, C2 1s ($2a_1$, $3a_1$) $\rightarrow \pi^*$ will occur at lower energy and with greater intensity, followed by a series of C 1s $\rightarrow$ valence and Rydberg transitions.

In the electronic configuration of trifluoropropyne, the lowest-energy orbitals are F 1s (1e, $1a_1$), which are much lower in energy than the carbon 1s ($2a_1$, $3a_1$, $4a_1$) orbitals and are not shown in Figure 2. From Figure 2, we can see that the C3 1s MO is much lower in energy than the other two carbon core orbitals. This results in the significant shift to higher energy observed in the TIY spectrum for excitations from the fluorinated carbon. The C1 and C2 MOs are very close in energy, and the sequence of these two orbitals is reversed compared to that of propyne. In addition, unlike the highly localized C1, C2 1s orbitals in propyne, there is a small amount of mixing between the C1 and C2 1s orbitals in trifluoropropyne. Nevertheless, it remains reasonable to describe the $3a_1$ and $4a_1$ MOs of trifluoropropyne as primarily localized on C1 and C2, respectively. In contrast to propyne, the unoccupied π^* (6e) in trifluoropropyne has no significant $\sigma^*_{CF_3}$ character. This decreased mixing between C1 and C2 on one hand and C3 and F on the other can be attributed to the larger energy difference between C−C π^* and C−F σ^* than between C−C π^* and C−H σ^*.

In propargyl alcohol, the lowest-energy MO is O 1s (1a′), followed by C3, C2, and C1 1s (2a′, 3a′, and 4a′) MOs. As in trifluoropropyne, the addition of an electronegative substituent on C3 results in a lowering of this MO energy relative to that of propyne, although as would be expected the effect of a single oxygen is less than that of three fluorines. The lower C_s symmetry of propargyl alcohol causes a splitting of the degenerate e-symmetry π^* MOs of propyne and trifluoropropyne into an out-of-plane a″-symmetry MO (4a″) and an in-plane a′-symmetry MO (16a′). The unoccupied π^* (4a″, 16a′) MOs are otherwise similar to the π^* orbitals of propyne, with π_{C2-C3} bonding and σ^*_{C3-OH}, σ^*_{C3-H} antibonding character in addition to the dominant $\pi^*_{C1\equiv C2}$ character.

Propyne. The TIY spectrum of propyne in the region below the C 1s ionization threshold is shown in Figure 3, along with our assignments. Both isotopically unmodified propyne and methyl-deuterated propyne were studied, with the primary motivation for the isotopic substitution being to allow differentiation between the methyl hydrogens and ethynyl hydrogen in a parallel study of the ionic fragmentation of propyne. No differences in the C 1s TIY spectra of the two samples were observed, indicating that none of the observed structure is attributable to excitation of C−H vibrational modes. The transition energies and term values of the features identified in

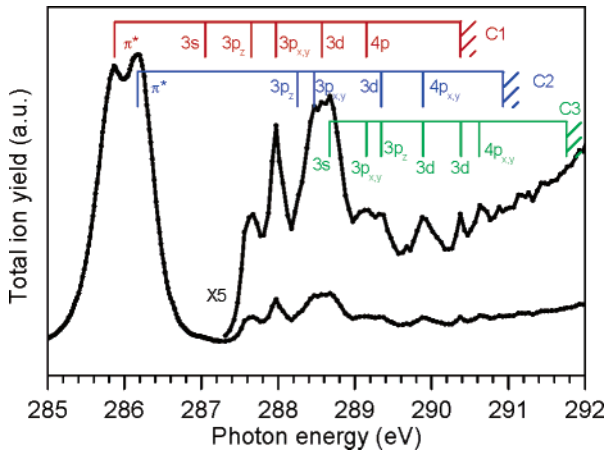

Figure 3. TIY spectrum of d_3-propyne near the C 1s ionization threshold. The hatched lines indicate the C 1s IPs.[8]

Figure 3 are listed in Table 1, along with the calculated term values and oscillator strengths and our assignments. The term values have been calculated using the experimental vertical ionization potentials reported by Sæthre et al.[8] Our calculated IPs, also listed in Table 1, are in good agreement with the experimental values, with the greatest difference 0.08 eV for C1. The assignments are based upon a combination of the experimental term values, our calculations, and comparison with the spectra of related molecules.

As shown in Figure 3, a strong band at about 286 eV, which is split into two peaks, dominates the C 1s TIY spectrum of propyne. These two peaks are attributed to C1, C2 1s → π^* (3e) transitions. The splitting between these two transitions is about 0.3 eV. This contrasts with the 0.56-eV splitting between the C 1s ionization potentials of C1 and C2 observed by Sæthre et al.[8] The difference in energy splitting for C 1s excitation versus C 1s ionization reflects the greater relaxation of the π^* (3e) MO in the presence of a core hole at C2 than at C1, partially offsetting the difference in the IPs. This is reflected in the greater term value, both experimental and calculated, for the C2 1s → π^* (3e) transition than for the C1 1s → π^* (3e) transition. This is also consistent with the greater calculated oscillator strength for the transition from C2 than from C1 (0.064 compared with 0.052). The larger oscillator strength indicates greater overlap between the C 1s hole and the upper π^* (3e) MO, which would also result in a larger energy lowering of the π^* (3e) MO in the presence of the C 1s hole. Following the strong C 1s → π^* transitions are a series of Rydberg transitions, which are much weaker because they are associated with excitation to more diffuse Rydberg orbitals. The p-type Rydberg orbitals split into two groups: p_z (a_1) along the symmetry axis and $p_{x,y}$ (e) perpendicular to the symmetry axis. The d-type Rydberg orbitals can split into three groups: d_z^2 (a_1), d_{xy}, $d_{x^2-y^2}$ (e), and d_{xz}, d_{yz} (e). Our calculations indicate that the oscillator strengths of the d-Rydberg transitions of propyne increase by the sequence of $d_z^2 < d_{xz}, d_{yz} < d_{xy}, d_{x^2-y^2}$.

If we think of propyne as methyl-substituted ethyne, then it is expected that the propyne spectrum should resemble the spectra of methane and ethyne according to Stöhr's building-block principle[2]. In ethyne, the two carbons are equivalent. Substitution of one of the hydrogen atoms with a methyl group will destroy the equivalency. The lower symmetry causes the splitting of the C 1s → π^* transition into two peaks, and the methyl-substituted carbon has the bigger chemical shift compared with ethyne. A comparison between the EELS,[24] high-resolution photoabsorption[25,26] and angle-resolved ion yield[27,28] spectra of C_2H_2 and our spectrum of propyne supports this qualitative interpretation. In C_2H_2, the spectrum is dominated by a single strong C 1s → π^* transition at 285.9 eV, followed by a series of Rydberg transitions. In the present spectrum of propyne, the C1 1s → π^* transition of the terminal ethynyl carbon has the transition energy of 285.87 eV, unchanged from that of C_2H_2. The C2 1s → π^* transition of the methyl-substituted carbon is shifted to the higher photon energy: 286.17 eV. It is interesting to note that, although the C1 1s → π^* transition energy in propyne is unchanged from that in ethyne,

TABLE 1: Energies, Term Values, Effective Principal Quantum Numbers (n^*), and Assignments of the C 1s Spectrum of Propyne

	experimental term value[b] (n^*) eV			calculated term value (T) and oscillator strength (f)						assignment		
energy[a] (eV)	C1	C2	C3	T_1 (n^*)	$f_1 \times 100$	T_2 (n^*)	$f_2 \times 100$	T_3 (n^*)	$f_3 \times 100$	C1	C2	C3
285.87	4.50(1.74)			2.67(2. 26)	5.179					π^*		
286.17		4.76(1.69)				3.16(2.07)	6.362				π^*	
287.05	3.32(2.02)			2.89(2.17)	0.002					3s		
287.65	2.72(2.23)	3.28(2.04)	4.11(1.82)	2.25(2.46)	0.039	2.88(2.17)	0.000			$3p_z$	3s	
287.97	2.40(2.38)	2.96(2.14)	3.79(1.90)	2.06(2.57)	0.563					$3p_x$,p_y		
288.26	2.11(2.54)	2.67(2.26)	3.50(1.97)			2.26(2.45)	0.003				$3p_z$	
288.47	1.90(2.67)	2.46(2.35)	3.29(2.04)	1.63(2.89)	0.014	1.91(2.67)	0.546			$3d_{z2}$	$3p_x$, p_y	
288.57	1.80(2.75)	2.36(2.40)	3.19(2.07)	1.38(3.15)	0.067					$3d_{xz}$, d_{yz}		
288.67	1.70(2.83)	2.26(2.45)	3.09(2.10)	1.34(3.19)	0.117			3.34(2.02)	0.036	$3d_{xy}$, d_{x2-y2}		3s
				1.32(3.21)	0.003					4s		
289.15	1.22(3.33)	1.78(2.77)	2.61(2.29)	1.08(3.54)	0.011	1.64(2.88)	0.001	2.38(2.39)	0.449	$4p_z$	$3d_{z2}$	$3p_x$, p_y
				1.07(3.57)	0.042					$4p_x$, p_y		
289.34	1.03(3.63)	1.59(2.93)	2.42(2.37)			1.40(3.12)	0.031	2.13(2.53)	0.005		$3d_{xz}$, d_{yz}	$3p_z$
						1.37(3.15)	0.110				$3d_{xy}$, d_{x2-y2}	
						1.32(3.21)	0.000				4s	
289.89	0.48(5.30)	1.04(3.62)	1.87(2.70)			1.10(3.52)	0.001	1.59(2.92)	0.014		$4p_z$	$3d_{z2}$
						1.04(3.62)	0.041	1.55(2.96)	0.145		$4p_x$,p_y	$3d_{xy}$, d_{x2-y2}
290.374[b]										IP		
290.38		0.55(4.98)	1.38(3.15)					1.41(3.11)	0.001			4s
								1.40(3.12)	0.029			$3d_{xz}$, d_{yz}
290.29[c]										IP		
290.62			1.14(3.46)					1.17(3.40)	0.159			$4p_x$, p_y
								1.07(3.56)	0.003			$4p_z$
290.929[b]											IP	
290.88[c]												
291.755[b]												IP
291.72[c]												

[a] Estimated absolute uncertainty ±0.1 eV. [b] Using the IPs reported in ref 8. [c] Calculated IPs.

the C1 vertical IP in propyne is 0.88 eV lower than the C 1s IP in ethyne, while the C2 1s IP differs from that in ethyne by only 0.32 eV.[8]

Following the C1, C2 1s → π^* transitions is a weak peak located at 287.65 eV, with a C1 term value of 2.72 eV ($n^* = 2.23$). The quantum defect, δ, of this transition is 0.77, which is reasonable for a p-type Rydberg transition. Hitchcock and Brion assigned the first weak peak in the ethyne ISEELS spectrum to the C 1s → 3s transition (TV = 3.1 eV, $\delta = 0.81$).[24] According to our calculations, the oscillator strength of the C1 1s → 3s (a_1) transition in propyne is very weak, only 0.00002; we give this assignment to the very weak peak at 287.05 eV, which has a term value relative to the 287.65 eV transition that is consistent with the calculated relative term values of the C1 1s → 3s and 1s → $3p_z$ transitions. The quantum defect of 0.98 is consistent with that of the C 1s → 3s transition of ethyne observed in the photoabsorption and angle-resolved ion yield studies.[25−28] Therefore, we assign the peak at 287.05 eV as C1 1s → 3s (a_1) and that at 287.65 eV as C1 1s → $3p_z$ (a_1), with a calculated oscillator strength of 0.0004. Our calculations place the C2 1s → 3s (a_1) transition at essentially the same energy as the C1 1s → $3p_z$ (a_1) transition, but with such a low oscillator strength (0.0000002) that experimental observation is not likely. The next most intense transitions after the C 1s → π^* are the C1, C2 1s (a_1) → $3p_{x,y}$ (e) transitions with calculated oscillator strengths of 0.0056 and 0.0055, respectively. The calculated relative position and relative intensity are consistent with the experimental peaks at 287.97 and 288.47 eV, although the quantum defects are underestimated in the calculation. The peak at 287.97 eV is assigned as C1 1s (a_1) → $3p_{x,y}$ (e). The broader band centered at 288.6 eV is assigned to overlapping C2 1s (a_1) → $3p_{x,y}$ (e) and C1 1s (a_1) → 3d transitions, with the weak shoulder on the low-energy side assigned as C2 1s (a_1) → $3p_z$ (a_1). On the basis of the quantum defects, the remaining transitions are assigned as indicated in Figure 3 and Table 1. The experimental quantum defects of the p Rydberg series are thus 0.62−0.77, while the experimental quantum defects of the d Rydberg series are 0.07−0.33. Our calculations consistently underestimate the term values and quantum defects of the Rydberg excitations; the quantum defects of the p-type Rydberg states are too low by 0.2−0.3, while those of the d-type Rydberg states are too low by 0.2−0.4. However, the relative energy spacing and intensities are consistent between experiment and theory.

Comparison of the spectrum of propyne with that of methane[29] further supports our assignments. The C 1s IP of CH_4 has been reported as 290.707 eV[30] and 290.689 eV,[31] and the C3 1s IP of propyne is 291.717 eV.[8] The substitution of hydrogen with an ethynyl group causes the IP to shift to a higher energy by ~1 eV. Therefore, as a first approximation, we expect the C3 transitions would also shift to higher photon energies by ~1 eV. The first two peaks in the spectrum of CH_4 were assigned to 3s+vib transitions with transition energies of 287.05 and 287.40 eV,[29] which correspond to the peak at 288.6 eV in propyne. The peak at 289.15 eV (TV = 2.61, $\delta = 0.71$) in propyne corresponds to peak 3 in CH_4, assigned as 3p (e) (TV = 2.72, $\delta = 0.76$). The last three peaks are also shifted about 1 eV to higher photon energy in propyne compared with the corresponding transitions in CH_4.

Trifluoropropyne. Expanded views of the C 1s TIY spectra of trifluoropropyne are shown in Figure 4. The experimental and calculated transitions are listed and compared in Table 2. The experimental term values were calculated using the literature ionization potentials.[8] The IPs calculated in this work are very

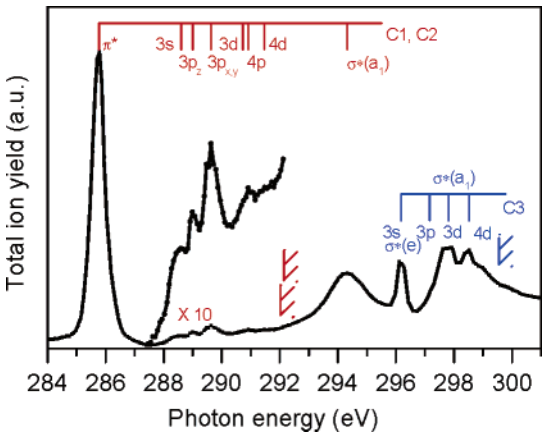

Figure 4. TIY spectrum of trifluoropropyne near the C 1s ionization thresholds. The hatched lines represent the reported C 1s IPs.[8]

similar to the experimental ones, although the ordering of our calculated C1 and C2 IPs of trifluoropropyne (292.23 and 292.10 eV) is the reverse of that reported by Sæthre et al. (292.025 and 292.144 eV),[8] determined by fitting of calculated vibrational profiles to the observed broad and relatively featureless band in the experimental photoelectron spectrum. Regardless of the correct ordering of these two IPs, the two studies are in general agreement both as to the magnitude of the IPs and that the difference between them is quite small. In both cases, these small differences in ionization energies cannot be unambiguously distinguished in the experimental spectrum. In the present work, because the C1 and C2 IPs are very similar, their transitions are expected to overlap each other. Because of the high electronegativity of fluorine, the IPs of C1 and C2 of trifluoropropyne are shifted to higher photon energy by about 1.65 and 1.22 eV, respectively, compared with those of propyne (290.374 and 290.929 eV).[8] However, the C1, C2 1s → π^* transition energies of trifluoropropyne do not show chemical shifts to higher energy as do the IPs. In contrast, the transition energies of C1, C2 1s (a_1) → π^* (6e) in trifluoropropyne shift to slightly lower energies compared with those of propyne. It is mentioned above that the calculated unoccupied π^* MO of trifluoropropyne differs from that of propyne. In propyne, the π^* (3e) MO is somewhat delocalized onto the methyl carbon C3, with π_{C3-C2} and $\sigma^*_{CH_3}$ character. In contrast, the π^* (6e) MO of trifluoropropyne has no significant $\sigma^*_{CF_3}$ character, and the electron density is therefore more closely localized around C1 and C2. This decreased interaction between the ethynyl carbons and the trifluoromethyl carbon is also reflected in the C2−C3 bond length of trifluoropropyne (1.470 Å), which is slightly longer than that in propyne (1.466 Å). Because the $\pi^*_{C1\equiv C2}$ MO is more localized around C1 and C2 in trifluoropropyne, the overlap between the $\pi^*_{C1\equiv C2}$ MO and the C1, C2 1s MOs is larger than in propyne. Consequently, when the core hole is formed, the energies of the $\pi^*_{C1\equiv C2}$ orbitals are lowered more in trifluoropropyne than in propyne. This is reflected in the significantly larger C 1s → π^* term values, both experimental and calculated, in trifluoropropyne relative to propyne, and in somewhat larger calculated oscillator strengths. Therefore, the overall effect on the excitation energies is a small shift to lower energy in trifluoropropyne. This illustrates the significant difference between the excitation spectra and ionization spectra: ionization spectra focus on the core-level orbital energy and relaxation of the core ionized molecule, whereas excitation spectra reflect not only the core orbital energy changes, but also the unoccupied valence shell orbital energy changes during the excitation process resulting from interaction between the core

TABLE 2: Energies, Term Values, Effective Principal Quantum Numbers (n^*), and Assignments of the C 1s Spectrum of Trifluoropropyne

	experimental term value[b] (n^*) eV			calculated term value (T) and oscillator strength (f)						assignment		
energy eV[a]	C1	C2	C3	$T_1(n^*)$	$f_1 \times 100$	$T_2(n^*)$	$f_2 \times 100$	$T_3(n^*)$	$f_3 \times 100$	C1	C2	C3
285.76	6.26(1.47)	6.38(1.46)		4.58(1.72)	6.940	4.70(1.70)	6.463			π^*	π^*	
288.60	3.42(1.99)	3.54(1.96)		3.11(2.09)	0.015	3.22(2.06)	0.001			3s	3s	
289.00	3.02(2.12)	3.14(2.08)		2.35(2.41)	0.073	2.35(2.41)	0.019			$3p_z$	$3p_z$	
289.46	2.56(2.30)	2.68(2.25)		2.21(2.48)	0.166					$3p_x$, p_y		
289.63	2.40(2.38)	2.51(2.33)				2.16(2.51)	0.047				$3p_x$, p_y	
290.27	1.76(2.78)	1.87(2.69)		1.54(2.97)	0.005	1.50(3.01)	0.006			$3d_{z2}$	$3d_{z2}$	
				1.40(3.11)	0.004	1.39(3.13)	0.004			$3d_{xy,}d_{x2-y2}$	4s	
				1.38(3.13)	0.012	1.38(3.14)	0.003			4s	$3d_{xy,}d_{x2-y2}$	
290.73	1.30(3.24)	1.41(3.10)		1.33(3.20)	0.112	1.27(3.27)	0.073			$3d_{xz,}$ d_{yz}	$3d_{xz,}$ d_{yz}	
290.91	1.12(3.49)	1.23(3.32)		1.12(3.48)	0.020	1.12(3.48)	0.004			$4p_z$	$4p_z$	
				1.12(3.49)	0.043	1.11(3.50)	0.001			$4p_x$, p_y	$4p_x$, p_y	
291.30	0.73(4.33)	0.84(4.01)		0.85(4.01)	0.003	0.83(4.05)	0.004			$4d_{z2}$	$4d_{z2}$	
291.47	0.56(4.95)	0.67(4.49)		0.79(4.16)	0.001	0.77(4.20)	0.002			$4d_{xy,}d_{x2-y2}$	$4d_{xy,}d_{x2-y2}$	
				0.73(4.32)	0.072	0.69(4.45)	0.049			$4d_{xz,}$ d_{yz}	$4d_{xz,}$ d_{yz}	
292.025[b]										IP		
292.23[c]												
292.144[b]											IP	
292.10[c]												
294.32	−2.3									σ^*		
296.18			3.37(2.01)					2.73(2.23)	0.179			3s
								2.72(2.24)	2.766			σ^*(e)
297.16			2.39(2.39)					2.06(2.57)	0.000			$3p_z$
								1.98(2.62)	0.000			$3p_x$,p_y
297.82			1.73(2.81)					1.53(2.98)	0.076			$3d_{z2}$
								1.34(3.19)	0.043			$3d_{xy,}$ d_{x2-y2}
								1.28(3.26)	0.062			4s/$\sigma^*(a_1)$
								1.27(3.27)	0.095			$3d_{xz,}$ d_{yz}
298.52			1.03(3.64)					1.03(3.63)	0.000			$4p_z$
								1.03(3.64)	0.000			$4p_x$,p_y
								0.84(4.03)	0.062			$4d_{z2}$
								0.74(4.28)	0.028			$4d_{xy,}d_{x2-y2}$
								0.70(4.41)	0.025			$4d_{xz,}$ d_{yz}
299.548[b]												IP
300.40[c]												

[a] Estimated absolute uncertainty ±0.1 eV. [b] Using the experimental IPs of ref 8. [c] Calculated IPs.

hole and the singly occupied valence MO. The C1, C2 1s (a_1) → π^* (6e) transitions of trifluoropropyne do not split as do the C1, C2 1s (a_1) → π^* (3e) transitions of propyne, because the C2 1s → π^* transition is shifted with fluorination at C3 more than the C1 1s → π^* transition, causing the two peaks to overlap in the spectrum. In essence, the differences in C1 and C2 1s → π^* term values and in the C1 and C2 IPs observed in propyne are negligible in trifluoropropyne. This superposition is reproduced by the calculations, which predict the two π^* transitions to be within 0.01 eV of each other and of very similar intensity. The remaining C1, C2 1s excitation features up to the C1, C2 1s ionization threshold at ∼292 eV are assigned to Rydberg transitions as indicated in Figure 4 and Table 2, on the basis of quantum defects and comparison with the calculated results.

The TIY spectrum of trifluoropropyne in the C3 1s excitation region is very different from that of propyne, as shown most clearly in Figure 1. The C 1s excitations from the fluorinated carbon are shifted to higher photon energy (294−299 eV) in trifluoropropyne due to the high electronegativity of fluorine. The highly electronegative fluorine atoms draw the electron density to fluorine, making C3 more positive and therefore requiring greater energy to excite a C3 1s electron. From comparison between the TIY spectra of propyne and trifuoropropyne, the broad peak at 294.3 eV in trifluoropropyne is assigned as the $\sigma^*_{C1\equiv C2}$ shape resonance of the ethynyl carbons, corresponding to the broad peak at 293.5 eV in propyne. A weak shoulder is observed at 294.80 eV on the $\sigma^*_{C1\equiv C2}$ shape resonance in trifluoropropyne. This was assigned as a C3 1s → π^*cc transition by Okada et al.,[11,32] but our calculations do not predict any such transition, and no C3 transitions near this photon energy.

To aid in the assignment of the C3 excitation features in the C 1s spectrum of trifluoropropyne, a comparison of the $-C^*F_3$ 1s spectrum of trifluoropropyne with those of CHF_3 and CF_4 [33,34] is employed. A broad "double peak" followed or overlapped with fine structures dominate the TIY spectra of CHF_3 and CF_4. The broad double peak was assigned to C 1s → σ^*_{C-F} transitions, whereas the fine structures correspond to the Rydberg transitions.[34] The σ^*_{C-H} antibonding orbitals in both propyne and trifluoropropyne are located above the corresponding ionization potentials, whereas the σ^*_{C-F} orbitals are located below the fluorinated carbon IP. Kosugi et al. have explained this in terms of the electron affinities of the atoms involved:[35] the electron affinity of F is much lower than that of C and H (3.399 eV for F, 1.263 for C, and 0.754 for H), and the C−F bond is weaker than the C−H bond (bond lengths are 1.336 and 1.084 Å, respectively). Moreover, calculation of the MOs in BF_3 indicates clearly the existence of barriers localized on the outer rim of the F atoms.[36] The barriers separate the excited states into inner-well and outer-well states. Inner-shell excitations to the inner-well states are intense because they can overlap strongly with the core hole. The broad transition is caused by tunneling through the barrier.[37]

Ueda et al. compared the TIY spectra of CH_4, CH_3F, CH_2F_2, CHF_3, and CF_4.[34] They found that when the hydrogen atoms are substituted by fluorine one by one, there is a gradual change from Rydberg-like transitions to σ^*_{C-F} transitions. In CF_4, the narrow Rydberg transitions are overlapped with the broad σ^*_{C-F} transition. In the present case of trifluoropropyne, although C3

has three fluorine substituents, the HC1≡C2 substituent also has an effect on the C3 core hole. From our calculated MOs of trifluoropropyne, we find strong valence antibonding orbitals delocalized around the carbon and fluorine atoms. Because of the expanded valence orbital size, the Rydberg orbitals may mix more with the valence orbitals, causing the valence orbitals to be trapped more with Rydberg transitions than in CF_4.

Trifluoropropyne has C_{3v} symmetry, so the C 1s → σ^*_{C-F} transitions will split into a_1-symmetry and e-symmetry as in CHF_3. The MO calculations indicate that the σ^*_{C-F} (e) orbital mixes with some C1≡C2 π character, lowering the energy of the σ^*_{C-F} (e) MO and increasing the splitting between the e-symmetry and a_1-symmetry σ^*_{C-F} MOs, as compared with CHF_3 and CF_4. The calculations reproduce the C3 σ^*_{C-F} and Rydberg transitions quite well, with quantum defects in agreement with the experimental results, allowing for the consistent underestimation in the calculations of the quantum defects by ~0.3, as noted above for propyne. The relatively narrow peak at 296.18 eV is therefore assigned as a combination of C3 1s → σ^*_{C-F} (e) and C3 1s → 3s, which the calculations predict at nearly the same energy. The broad band at ~298 eV is assigned as C3 1s → σ^*_{C-F} (a_1), with superimposed structure from narrower Rydberg transitions, as also observed in CF_4.[34] The assignments given here differ from those provided in the previous photoabsorption and angle-resolved ion yield study of trifluoropropyne.[11] The differences in the assignment of the Rydberg transitions, which were also based largely on quantum defects in the previous study, are attributable to the differences between the estimated IPs, taken from Jolly et al.,[38] that were used in ref 11 (292.0, 292.5, 299.7 eV for C1, C2, and C3, respectively), and those used in this work, taken from ref 8 (292.025, 292.144, and 299.548 eV for C1, C2, and C3, respectively) and also to the ~0.8 eV difference in absolute energy scale between this work and that of ref 11. Okada et al. assigned the peak that is observed in the present study at 296.18 eV to a parallel C3 1s (a_1) → σ^*_{C-F} (a_1) transition on the basis of a positive anisotropy parameter determined by angle-resolved ion spectroscopy.[11] Our assignment of this peak as a combination of C3 1s → σ^*_{C-F} (e) and C3 1s → 3s is not inconsistent with the observed anisotropy parameter, if the angular dependence of the ion yields comes primarily from the C3 1s → 3s component of the excitation while the C3 1s → σ^*_{C-F} (e) excitation leads primarily to C−F bond dissociation, which would display little angular dependence because of the difference in orientation between the molecular symmetry axis and the C−F bond dissociation axis.

Propargyl Alcohol. The TIY spectrum of propargyl alcohol is presented in Figure 5. The experimental transition energies and term values, calculated term values and oscillator strengths, and assignments are listed in Table 3. As mentioned above, considerably greater structure is evident in the high-resolution spectrum reported here than in the previously reported EELS spectrum of propargyl alcohol.[9] Allowing for the difference in energy resolution, however, the two measurements are consistent.

In contrast to propyne and trifluoropropyne, we know of no reported determinations of the experimental C 1s IPs of propargyl alcohol. Considering the good agreement obtained between experiment and the calculated IPs of propyne and trifluoropropyne, we have used our calculated IPs for propargyl alcohol (290.54, 290.89, and 293.39 eV for C1, C2, and C3, respectively) to determine term values for the experimental transitions. Estimation of the IPs by comparison with known IPs of similar molecules further supports these calculated results.

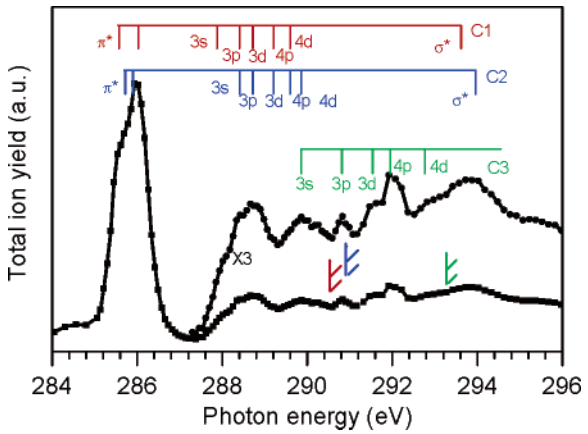

Figure 5. TIY spectrum of propargyl alcohol near the C 1s ionization thresholds. The hatched lines are the calculated C 1s IPs.

For example, the C3 IP can be estimated from the C 1s IPs of the substituted carbon in methanol and ethanol, 292.5 eV in both cases,[9] and the substitution effect of the ethynyl group, which increases the C 1s IP by ~1.0 eV on the basis of the comparison of methane and propyne, discussed above. This gives an estimated C3 1s IP of 293.5 eV, in good agreement with the calculated IP of 293.39 eV. A similar estimate is obtained if we start from the 291.75 eV C3 1s IP of propyne[8] and correct for the effect of OH substitution. On the basis of the IP difference between CH_3CH_3 (290.7 eV)[8] and CH_3CH_2-OH (292.5 eV),[9] substitution of H by OH causes an increase of ~1.8 eV in the C 1s IP, yielding an estimated C3 IP for propargyl alcohol of 293.55 eV.

Although the C1,C2 1s → π^* transition of propargyl alcohol is not split to the extent observed for propyne, it is broader than that of trifluoropropyne and has a shoulder at 285.57 eV on the low-energy side of a more intense transition at 285.98 eV. This is consistent with our calculations, which place the C1 1s → π^* (a′) transition 0.14 eV lower in energy than the C2 1s → π^* (a′), with calculated oscillator strengths of 0.025 and 0.029, respectively, followed by the C2 1s → π^* (a″) and C1 1s → π^* (a″) transitions, 0.33 and 0.45 eV to higher energy than the C1 1s → π^* (a′) transition and with respective oscillator strengths of 0.026 and 0.033. As was observed in C1 and C2 1s excitation to the same π^* level in propyne, there is a correlation between calculated term value and oscillator strength. The remaining peaks in the C 1s TIY spectrum of propargyl alcohol have been assigned to Rydberg excitations on the basis of experimental term values and our calculations. The assignments are indicated in Table 3 and in Figure 5. In propargyl alcohol, the moderate splitting between the C1 and C2 1s IPs (0.35 eV) and the lower symmetry result in the relatively broad peaks observed in the TIY spectrum, arising from the overlap of Rydberg series offset slightly in energy.

Summary and Conclusions

High-resolution C 1s excitation spectra of propyne, trifluoropropyne, and propargyl alcohol have been determined using TIY spectroscopy with narrow bandwidth synchrotron radiation. In the case of propyne and propargyl alcohol, this work represents a significant improvement in resolution over the previous EELS spectra,[2,9,10] revealing structure not previously observed. The measurement of the spectra of these three chemically related molecules under the same experimental conditions has allowed a detailed study of the electronic structure changes that occur with substitution of a simple hydrocarbon, propyne, with electronegative substituents, F and OH. The high

TABLE 3: Energies, Term Values, Effective Principal Quantum Numbers (n^*) and Assignments of the C 1s Spectrum of Propargyl Alcohol

	experimental term value[b] (n^*) eV			calculated term value (T) and oscillator strength (f)						assignment		
energy[a] eV	C1	C2	C3	$T_1(n^*)$	$f_1 \times 100$	$T_2(n^*)$	$f_2 \times 100$	$T_3(n^*)$	$f_3 \times 100$	C1	C2	C3
285.57	4.97(1.65)	5.32(1.60)		3.22(2.05)	2.538					$\pi^*(a')$		
						3.43(1.99)	2.895				$\pi^*(a')$	
285.98	4.56(1.73)	4.91(1.66)		2.77(2.22)	2.601	3.24(2.05)	3.290			$\pi^*(a'')$	$\pi^*(a'')$	
287.88	2.66(2.26)	3.01(2.13)		2.77(2.22)	0.228					3s		
288.40	2.14(2.52)	2.49(2.34)	4.99(1.65)	2.24(2.46)	0.120	2.80(2.20)	0.091			3p(a′)	3s	
				2.02(2.60)	0.312	2.24(2.46)	0.065			3p(a″)	3p(a′)	
				1.97(2.63)	0.007	2.00(2.61)	0.000			3p(a′)	3p(a′)	
288.71	1.83(2.73)	2.18(2.50)	4.68(1.71)	1.63(2.89)	0.052	1.89(2.69)	0.259			3d(a′)	3p(a″)	
				1.38(3.14)	0.057					3d(a″)		
				1.33(3.19)	0.048	1.68(2.85)	0.032			3d(a′)	3d(a′)	
				1.28(3.26)	0.057					3d(a′)		
				1.27(3.28)	0.009					3d(a″)		
				1.26(3.28)	0.045					4s		
289.20	1.34(3.19)	1.69(2.84)		1.09(3.54)	0.018					4p(a′)		
				1.06(3.58)	0.027	1.42(3.10)	0.048			4p(a″)	3d(a″)	
				1.02(3.65)	0.002	1.36(3.17)	0.082			4p(a′)	3d(a′)	
						1.30(3.23)	0.020				3d(a′)	
						1.28(3.26)	0.006				3d(a″)	
						1.27(3.27)	0.029				4s	
289.60	0.94(3.80)	1.29(3.25)		0.89(3.91)	0.015	1.10(3.52)	0.007			4d(a′)	4p(a′)	
				0.76(4.24)	0.024	1.04(3.62)	0.003			4d(a″)	4p(a′)	
				0.74(4.30)	0.017	1.03(3.64)	0.022			4d(a′)	4p(a″)	
				0.72(4.34)	0.016					4d(a′)		
				0.71(4.38)	0.009					4d(a″)		
289.86	0.68(4.47)	1.03(3.63)	3.53(1.96)			0.91(3.88)	0.008	3.44(1.99)	0.244		4d(a′)	3s
290.22	0.32(6.52)	0.67(4.51)	3.17(2.07)			0.77(4.20)	0.012				4d(a″)	
						0.74(4.28)	0.036				4d(a′)	
						0.73(4.33)	0.001				4d(a′)	
						0.71(4.37)	0.006				4d(a″)	
290.54[b]										IP		
290.81			2.58(2.30)					2.48(2.34)	0.059			3p(a′)
								2.47(2.35)	0.315			3p(a″)
								2.04(2.58)	0.036			3p(a′)
290.89[b]											IP	
291.53			1.86(2.70)					1.62(2.90)	0.128			4s/σ^*
								1.55(2.96)	0.041			3d(a′)
								1.43(3.08)	0.001			3d(a′)
								1.41(3.11)	0.005			3d(a″)
								1.37(3.15)	0.065			3d(a″)
								1.35(3.17)	0.000			3d(a′)
291.96			1.43(3.08)					1.21(3.35)	0.039			4p(a′)
								1.21(3.36)	0.085			4p(a″)
								1.05(3.60)	0.017			4p(a′)
292.77			0.62(4.68)					0.86(3.97)	0.016			4d(a′)
								0.80(4.13)	0.057			4d(a″)
								0.79(4.15)	0.000			4d(a′)
								0.77(4.20)	0.003			4d(a″)
								0.76(4.24)	0.001			4d(a′)
293.39[b]												IP
293.78										σ^*		

[a] Estimated absolute uncertainty ±0.1 eV. [b] Calculated IPs.

resolving power has allowed comparison not only of similar excitations between molecules (e.g., C 1s → π^*), but also similar excitations within the same molecule but from chemically inequivalent carbon centers (e.g., C1 1s ($3a_1$) → π^* (3e) vs C2 1s ($2a_1$) → π^* (3e) of propyne).

Consideration of ground-state MO energies, both inner-shell and unoccupied valence, provides some insight into the effects of electronegative substitution and the likely C 1s transitions, but does not provide a quantitative picture of the C 1s excitation spectroscopy owing to the significant and state-specific electronic relaxation effects that occur in the presence of a C 1s hole. In contrast, calculation of the C 1s ionized states with explicit consideration of the inner-shell hole and calculation of the C 1s excited states using the IVO method provides a quantitative description of the C 1s excitation processes. Accurate C 1s ionization potentials were obtained, typically differing from the experimental values for propyne and trifluoropropyne by less than 0.10 eV. The worst agreement was for the fluorinated carbon C3 1s IP of trifluoropropyne, where experiment and theory differed by 0.84 eV. In the case of C 1s excitation, the calculated term values consistently underestimated the experimental values, by a few tenths of an eV in the case of Rydberg excitations and ~1.5 eV in the case of C 1s → valence excitation. However, the relative ordering and intensities of the calculated C 1s excitations were in good agreement with experiment; the calculations were therefore of significant utility in assigning and interpreting the spectra. The poorer accuracy of the calculated term values of the valence transitions may be a consequence of the failure of the IVO method to account for interactions between the singly excited electron and the other

valence electrons in the excited state. This error would be largest for the more compact valence excited states and less significant for Rydberg states.

The spectral changes observed in these molecules with changes in substituent can be broadly classified in two categories. For Rydberg transitions, the transition energies tend to shift with the corresponding IPs, shifting to higher energy with the addition of electronegative substituents such as F and OH. Consequently, the term values and quantum defects of the Rydberg transitions change little between carbon centers, whether in the same or different molecules. In contrast, the C 1s excitations to low-lying valence states exhibit only very small changes in transition energy with changes in substituent, even when the corresponding C 1s IPs exhibit large shifts. Consequently, the term values of the C 1s-valence excitations vary considerably, depending upon the electronic environment of the core excited atom. These two different behaviors can be understood qualitatively in terms of the extent of interaction between the C 1s hole and the singly occupied upper level. In the case of C 1s $\rightarrow$ valence excitation, interaction can be substantial and significant electronic relaxation occurs in the upper valence level. Those circumstances giving rise to increased C 1s-valence interaction, that is, decreased electrostatic shielding of the nuclear charge by addition of electronegative substituents, also cause a corresponding shift in the C 1s IPs. In contrast, the Rydberg levels are considerably more diffuse than the valence levels and therefore interact less with the compact C 1s hole. Changes in the electronic environment of the core excited atom therefore have less impact on the energy of the Rydberg level. The behavior of the C 1s-valence excitations leads to effects that at first appear counter-intuitive. For example, the C1 1s IP of trifluoropropyne is shifted 1.65 eV to *higher* energy compared with the C1 1s IP of propyne, but the C1 1s $\rightarrow \pi^*$ transition of trifluoropropyne is shifted 0.11 eV to *lower* energy relative to the C1 1s $\rightarrow \pi^*$ transition of propyne.

In general, the inner-shell excitations are a sensitive probe of LUMO character. For example, for both propyne and propargyl alcohol, the C1 1s $\rightarrow \pi^*$ transitions have somewhat lower intensities than the C2 1s $\rightarrow \pi^*$ transitions. From our calculations, it is found that the unoccupied $\pi^*_{C1\equiv C2}$ MOs of propyne and propargyl alcohol are mixed with some π_{C2-C3} contributions, resulting in greater electron density around C2 than C1. Consequently, the overlap of the C2 1s hole with the π^* MO is greater than that of the C1 1s hole, leading to a greater oscillator strength.

With inner-shell spectroscopy, literature ionization potentials, and ab-initio theoretical calculations, we are able to gain insight into the substituent effects of ethynyl, trifluoromethyl, and hydroxide. The substituent effects of these electronegative groups affect not only the core hole, which plays a large role in determining the ionization potentials, but also affect the unoccupied valence orbitals and the interaction between the core hole and the unoccupied valence orbitals. This makes the core excitation spectra a rich and complex avenue for exploration of valence electronic structure as well as of the inner-shell levels themselves.

Acknowledgment. Financial support was provided by NSERC. SRC is funded by the NSF (DMR-0084402). We thank the CSRF personnel for their assistance, in particular Yong Feng Hu.

References and Notes

(1) Hitchcock, A. P. *Phys. Scr.* **1990**, *T31*, 159.

(2) Stöhr, J. *NEXAFS Spectroscopy*; Springer-Verlag: Berlin, 1992.

(3) Kiefer, J. H.; Kumaran, S. S.; Mudipalli, P. S. *Chem. Phys. Lett.* **1994** *224*, 51−55.

(4) Shieh, J.-C.; Wu, J.-C.; Li, R.; Mebel, A. M.; Handy, N. C.; Chen, Y.-T. *J. Chem. Phys.* **2000**, *112*, 7384.

(5) Qadiri, R. H.; Feltham, E. J.; Cottill, E. E. H.; Taniguchi, N.; Ashfold, M. N. R. *J. Chem. Phys.* **2002**, *116*, 906.

(6) Sun, W.; Yokoyama, K.; Robinson, J. C.; Suits, A. G.; Neumark, D. M. *J. Chem. Phys.* **1999**, *110*, 4363.

(7) Cavell, R. G. *J. Electron Spectrosc. Relat. Phenom.* **1975**, *6*, 281−296.

(8) Sæthre, L. J.; Berrah, N.; Bozek, J. D.; Børve, K. J.; Carroll, T. X.; Kukk, E.; Gard, G. L.; Winter, R.; Thomas, T. D. *J. Am. Chem. Soc.* **2001**, *123*, 10729−10737.

(9) Ishii, I.; Hitchcock, A. P. *J. Electron Spectrosc. Relat. Phenom.* **1988**, *46*, 55−84.

(10) Hitchcock, A. P.; Mancini, D. C. *J. Eectron Spectrosc. Relat. Phenom.* **1994**, *67*, 1−123. Most recent version: http://unicorn.mcmaster.ca/corex/ cedb-title.html .

(11) Okada, K.; Tanimoto, S.; Ibuki, T.; Haga, Y.; Gejo, T.; Saito, K.; Ohno, K. *Chem. Phys.* **2004**, *304*, 273−279.

(12) Yates, B. W.; Hu, Y. F.; Tan, K. H.; Retzlaff, G.; Cavell, R. G.; Sham, T. K.; Bancroft, G. M. *J. Synchrotron Radiat.* **2000**, *7*, 296.

(13) Hitchcock, A. P.; Neville, J. J. In *Chemical Applications of Synchrotron Radiation*; Sham, T. K., Ed.; World Scientific: Singapore, 2001.

(14) Guerra, A. C. O.; Maciel, J. B.; Turci, C. C.; Bilodeau, R. C.; Hitchcock, A. P. *Can. J. Chem.* **2004**, *82*, 1052−1060.

(15) Wiley, W. C.; McLaren, I. H. *Rev. Sci. Instrum.* **1955**, *26*, 1150.

(16) Henke, L.; Gullikson, E. M.; Davis, J. C. *At. Data Nucl. Data Tables* **1993**, *54*, 181−342

(17) Saito, N.; Heiser, F.; Hemmers, O.; Wieliczek, K.; Viefhaus, J.; Becker, U. *Phys. Rev. A* **1996**, *54*, 2004.

(18) Schmidt, M. W.; Baldridge, K. K.; Boatz, J. A.; Elbert, S. T.; Gordon, M. S.; Jensen, J. H.; Koseki, S.; Matsunaga, N.; Nguyen, K. A.; Su, S. J.; Windus, T. L.; Dupuis, M.; Montgomery, J. A. *J. Comput. Chem.* **1993**, *14*, 1347−1363.

(19) Kosugi, N.; Kuroda, H. *Chem. Phys. Lett.* **1980**, *74*, 490−493.

(20) Hunt, W. J.; Goddard, W. A., III. *Chem. Phys. Lett.* **1969**, *3*, 414.

(21) Huzinaga, S.; Andzelm, J.; Klobukowski, M.; Andzelm, E. R.; Sakai, Y.; Tatewaki, H. *Gaussian Basis Sets for Molecular Calculations*; Elsevier: Amsterdam, 1984.

(22) Krishnan, R.; Binkley, J. S.; Seeger, R.; Pople, J. A. *J. Chem. Phys.* **1980**, *72*, 650.

(23) Kaufmann, K.; Nager, Ch.; Jungen, M. *Chem. Phys.* **1985**, *95*, 385.

(24) Hitchcock, A. P.; Brion, C. E. *J. Electron Spectrosc. Relat. Phenom.* **1977**, *10*, 317.

(25) Ma, Y.; Chen, C. T.; Meigs, G.; Randall, K.; Sette, F. *Phys. Rev. A* **1991**, *44*, 1848−1858.

(26) Kivimäki, A.; Neeb, M.; Kempgens, B.; Köppe, H. M.; Maier, K.; Bradshaw, A. M. *J. Phys. B*: *At. Mol. Opt. Phys.* **1997** *30* 4279−4291.

(27) Adachi, J.; Kosugi, N.; Shigemasa, E.; Yagishita, A. *Chem. Phys. Lett.* **1999**, *309*, 427−433.

(28) Masuda, S.; Gejo, T.; Hiyama, M.; Kosugi, N. *J. Electron Spectrosc. Relat. Phenom.* **2005**, *144−147*, 215−218.

(29) Ueda, K.; Okunishi, M.; Chiba, H.; Shimizu, Y.; Ohmori, K.; Sato, Y.; Shigemasa, E.; Kosugi, N. *Chem. Phys. Lett.* **1995**, *236*, 311−317.

(30) Asplund, L.; Gelius, U.; Hedman, S.; Helenelund, K.; Siegbahn, K.; Siegbahn, P. E. M. *J. Phys. B*: *At. Mol. Phys.* **1985**, *18*, 1569−1579.

(31) Myrseth, V.; Bozek, J. D.; Kukk, E.; Sæthre, L. J.; Thomas, T. D. *J. Electron Spectrosc. Relat. Phenom.* **2002**, *122*, 57−63.

(32) Ibuki, T.; Okada, K.; Tanimoto, S.; Saito, K.; Gejo, T. *J. Electron Spectrosc. Relat. Phenom.* **2002**, *123*, 323.

(33) Thomas, M. K.; Fisher, B. O.; Hatherly, P. A.; Codling, K.; Stankiewicz, M.; Roper, M. *J. Phys. B*: *At. Mol. Opt. Phys.* **1999**, *32*, 2611.

(34) Ueda, K.; Shimizu, Y.; Chiba, H.; Okunishi, M.; Ohmori, K.; Sato, Y.; Shigemasa, E.; Kosugi, N. *J. Electron Spectrosc. Relat. Phenom.* **1996**, *79*, 441.

(35) Kosugi, N.; Ueda, K.; Shimizu, T.; Chiba, H.; Okunishi, M.; Ohmori, K.; Sato, Y.; Shigemasa, E. *Chem. Phys. Lett.* **1995**, *246*, 475.

(36) Cadioli, B.; Pincelli, U.; Tosatti, E.; Fano, U.; Dehmer, J. L. *Chem. Phys. Lett.* **1972**, *17*, 15.

(37) Dehmer, J. L. *J. Chem. Phys.* **1972**, *56*, 4496.

(38) Jolly, W. L.; Bomben, K. D.; Eyermann, C. J. *At. Data Nucl. Data Tables* **1984**, *31*, 433.